HYDRODYNAMIC FUEL CONTAINMENT IN AN OPEN-CYCLE GAS CORE NUCLEAR ROCKET

David I. Poston and Terry Kammash
Department of Nuclear Engineering
University of Michigan
Ann Arbor, MI 48109
(313) 747-0900

Abstract

A thermal-hydraulic model of an open-cycle gas core nuclear rocket is used to examine the fuel containment characteristics of the system. A parametric analysis is performed which studies how the average containment time, average number density, and mass loading of the fuel vary as a function of several design and operational parameters. The containing effect of the injected fluids is studied by varying the velocity and injection angle of the outer wall flow. The effect of rocket acceleration on the containment of the fuel is also examined. The results offer both a qualitative and quantitative look at fuel containment, thereby providing another step toward establishing the feasibility, or lack thereof, of the open-cycle gas core nuclear rocket.

INTRODUCTION

The open-cycle Gas Core Nuclear Rocket (GCR) has the potential to deliver astounding rocket performance. Poston and Kammash (1992) found that if the fuel and propellant can be prevented from mixing, a 3000 MW reactor can produce a specific impulse of 3160 s with a thrust of 125 kN. However, the open-cycle GCR receives little attention because of many unanswered questions. The most elusive and potentially show-stopping of these questions is that of fuel containment.

In the GCR, a fissioning uranium plasma heats (primarily by radiation) a hydrogen propellant, which is exhausted through a choked nozzle. In the open-cycle GCR there is no physical barrier between the fuel and propellant; therefore, the flow field must be constructed in a manner which minimizes fuel/propellant mixing. The objective of this work is to provide insight as to how this might be achieved.

The thermal-hydraulic model used to perform this analysis is described in Poston and Kammash (1994). A numerical solution of the Navier-Stokes, energy, and species diffusion equations is obtained as a function of design and operational parameters. The fuel (uranium) and propellant (hydrogen) enter the reactor with a constant mass flow rate; the propellant surrounds the fuel in the shape of a cylindrical annulus. The propellant enters the reactor with a user-specified velocity profile, which includes: the inlet and wall mass flow rates, the buffer zone dimensions, and the injection velocity and angle of wall flow. If the maximum wall heat flux is reached, the propellant flow through the wall is increased to provide transpiration cooling. In addition to the flow rates, the system dimensions, material limitations, power, and boundary conditions are used as code input.

To study fuel containment a parametric analysis is performed. Fuel containment parameters such as fuel loading, confinement time, and number density, are calculated as a function of power, fuel mass flow rate, propellant mass flow rate, reactor dimensions, and the propellant flow profile. An optimum design is selected by weighing the fuel containment characteristics of the system versus the specific impulse and thrust. Special attention will be focused on how the hydrodynamic forces of the injected fluid compare to the forces generated by the expansion and mixing of the fluids. The effect of rocket acceleration on fuel containment is examined by adding an external force term to the axial momentum equation. Finally, a brief discussion of how turbulence modeling effects the solution will be presented.

ANALYSIS

In cylindrical geometry, the steady state conservation equations of mass, species, axial and radial momentum, and energy are (assuming azimuthal symmetry and axial external forces only):

$$\frac{\partial}{\partial z}(\rho v_z)+\frac{1}{r}\frac{\partial}{\partial r}(r\rho v_r)=0 \quad , \tag{1}$$

$$\frac{\partial}{\partial z}(\rho v_z y)+\frac{1}{r}\frac{\partial}{\partial r}(r\rho v_r y)=\frac{\partial}{\partial z}\left(\rho D_{1\text{-}2}\frac{\partial y}{\partial z}\right)+\frac{1}{r}\frac{\partial}{\partial r}\left(r\rho D_{1\text{-}2}\frac{\partial y}{\partial r}\right) \quad , \tag{2}$$

$$\rho v_z\frac{\partial v_z}{\partial z}+\rho v_r\frac{\partial v_z}{\partial r}=-\frac{\partial P}{\partial z}+\frac{\partial}{\partial z}\left(\mu\frac{\partial v_z}{\partial z}\right)+\frac{1}{r}\frac{\partial}{\partial r}\left(r\mu\frac{\partial v_z}{\partial r}\right)+\rho g_z \quad , \tag{3}$$

$$\rho v_z\frac{\partial v_r}{\partial z}+\rho v_r\frac{\partial v_r}{\partial r}=-\frac{\partial P}{\partial r}+\frac{\partial}{\partial z}\left(\mu\frac{\partial v_r}{\partial z}\right)+\frac{1}{r}\frac{\partial}{\partial r}\left(r\mu\frac{\partial v_r}{\partial r}\right) \quad , \tag{4}$$

$$\frac{\partial}{\partial z}(\rho v_z\overline{C_p}T)+\frac{1}{r}\frac{\partial}{\partial r}(\rho v_r\overline{C_p}T)+\sum_{i=1}^{2}\frac{\partial}{\partial z}\left(j_{zi}\overline{C_{pi}}T\right)+\sum_{i=1}^{2}\frac{1}{r}\frac{\partial}{\partial r}\left(j_{ri}\overline{C_{pi}}T\right)=\frac{\partial}{\partial z}\left(k\frac{\partial T}{\partial z}\right)+\frac{1}{r}\frac{\partial}{\partial r}\left(rk\frac{\partial T}{\partial r}\right)+Q_v\,. \tag{5}$$

The volumetric power generation Q_V is dependent on the fuel number density, which is representative of a constant neutron flux. The axial external force g_Z is included in order to study the effects of rocket acceleration. Thermal radiation is modeled with the diffusion approximation. The thermal radiation absorption coefficients of the fuel and propellant are sufficiently high to justify the use of the diffusion method (the propellant is seeded with high Z particles to aid in the absorption of radiation at low temperatures). The diffusion method models radiative heat transfer in the form of conduction, with a conduction coefficient depending on T^3. The total conductivity is:

$$k=k_{cond}+k_{rad}=k_c+\frac{16\sigma T^3}{3a_r} \quad . \tag{6}$$

The diffusion approximation is valid in all regions except near the wall, where optical thickness is low. An absorption integral is evaluated to more accurately predict the radiative component of the wall heat flux:

$$q_w=\frac{1}{r_w}\int_0^{r_w} r a_p\sigma T^4\exp\left\{-\int_r^{r_w} a_p dr'\right\}dr \quad . \tag{7}$$

The conductivity coefficient at the wall is iterated until the diffusion solution produces a radiative wall heat flux equal to the result of the absorption integral.

In order to improve the numerical stability of the model, a staggered grid approach is used. Because of this, boundary conditions for each of the five solution variables (T, Vz, Vr, P and y) are not required at each boundary. At the inlet, all variables are specified; the temperature and pressure are uniform, the radial velocity is zero, and the free stream values of axial velocity and concentration are connected by either a step or a ramp function. At the core centerline, radial velocity is zero, and symmetry applies to all other variables. At the outer wall, the temperature, radial velocity, injection area, injection angle, and concentration are all specified, and a slip condition is assumed for axial velocity. A boundary condition for pressure is not required since pressure is calculated on the outer radial edge of the mesh cell. Also at the wall a maximum heat flux is specified. If this value is exceeded, the flow from the wall is increased providing transpiration cooling. At the core exit, an extrapolation boundary condition is used for all variables, except axial velocity since it is calculated on the downstream edge of the mesh cell. An extrapolation boundary condition assumes that radial pressure variations due to nozzle convergence do not propagate back to the core exit. The only effect the nozzle has on the thermal-hydraulic solution is in the determination of the average reservoir pressure.

To shorten this report, many aspects of the model will not be discussed. A more detailed description of the model can be found in Poston and Kammash (1994), which provides a description of: the method of solution used to obtain convergence of the above equations, the turbulent modeling options offer by the code, the sources of fluid properties and how mixture properties are calculated, and how rocket performance (Isp and thrust) are calculated.

There are fifteen input parameters to the model which have an effect on fuel containment. To limit the scope of this paper six were chosen for parametric study: fuel mass flow rate, total propellant flow rate, wall propellant flow rate, reactor power, outer wall radius, and rocket acceleration. Also examined are the effect of the wall injection angle and velocity.

RESULTS AND DISCUSSION

A relatively low performance 500 MW GCR was chosen to serve as the anchor point for the parametric analysis. This design was selected because higher performance reactors (in terms of Isp and thrust) resulted in very low fuel densities and poor numerical stability. The input parameters and results for the base case are listed in Table 1. The thermal-hydraulic characteristics of the base case, such as temperature, velocity, and concentration profiles, are discussed in Poston and Kammash (1994).

TABLE 1. Input Parameters and Results for Base Case Open-Cycle GCR Design.

Input Parameters		Results	
Reactor Power (MW)	500	Fuel Reservoir Temp. (K)	34,400
Reactor Pressure (atm)	1000	Prop. Reservoir Temp. (K)	5,611
Inlet Prop. Flow Rate (kg/s)	3.0	Specific Impulse (s)	1,421
Wall Prop. Flow Rate (kg/s)	0.0	Thrust (kN)	55.7
Inlet Fuel Flow Rate (kg/s)	1.0		
Inlet Temperature (K)	2200	Average Fuel Density (#/m^3)	7.08E+24
Wall Temperature (K)	2200	Fuel Loading (kg)	42.0
Core Length (m)	2.00	Fuel Residence Time (s)	42.0
Fuel Radius at Inlet (m)	1.20	Prop. Loading (kg)	49.2
Buffer Zone Outer Rad. (m)	1.35	Prop. Residence Time (s)	16.4
Outer Wall Radius (m)	1.50		
Turbulence Model	none		

Results are graphed and discussed below for the following parameters: power, fuel mass flow, propellant mass flow, wall mass flow, outer wall radius, and rocket acceleration.

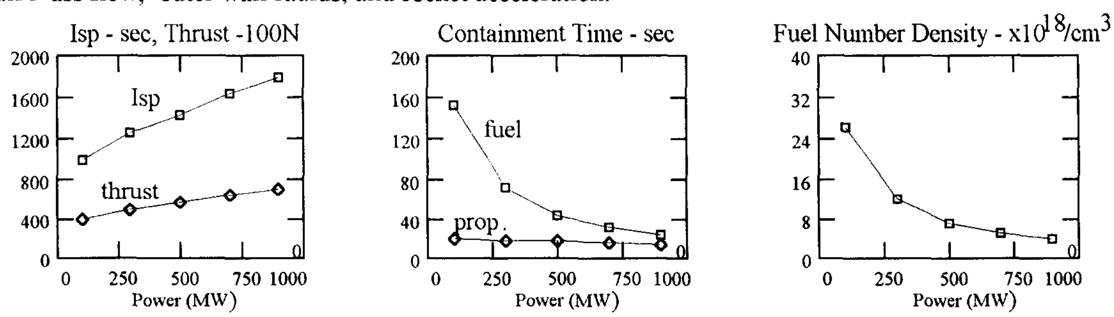

FIGURE 1. Reactor Power Varied.

As the reactor power is increased from 100 MW to 900 MW, the rocket performance is nearly doubled. In some respects, the performance is increased by a factor of four since both specific impulse and thrust are doubled. Unfortunately, this increase in performance is offset by a drastic drop in fuel containment. This drop in fuel density is not due to higher temperatures: as power increases from 100 MW to 900 MW the average fuel temperature increases by 30%, while the average fuel density decreases by 700%. Study of the thermal-hydraulics of each design shows that as the power increases, the convective currents within the reactor increase dramatically. The majority of fuel loss is caused by a massive influx of high momentum hydrogen into the fuel region. Another factor which promotes fuel loss, but not as important, is the axial acceleration of the fuel due to thermal expansion.

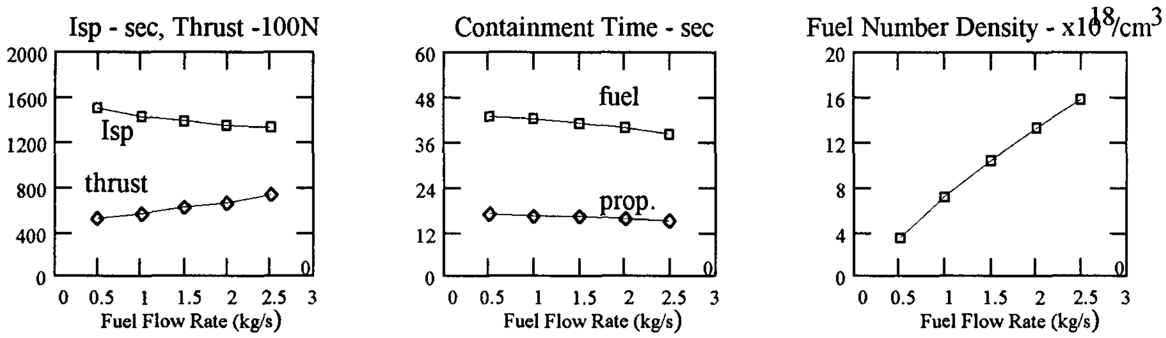

FIGURE 2. Fuel Mass Flow Rate Varied.

As the fuel mass flow rate is increased, there is a gain in thrust and a drop in specific impulse, due mainly to the high molecular weight of the fuel. The containment time of the fuel remains relatively constant, signifying that fuel containment is not highly dependent on inlet velocity. Obviously the big advantage of a high fuel flow rate is the gain in fuel density, which makes the task of achieving neutron criticality much easier. As the fuel flow rate increases, it becomes more difficult for the hydrogen to infiltrate the core, leaving a region of high purity uranium near the centerline. Of course the benefits of increasing the fuel flow rate (i.e. fuel leakage) have to be weighed against cost and safety considerations.

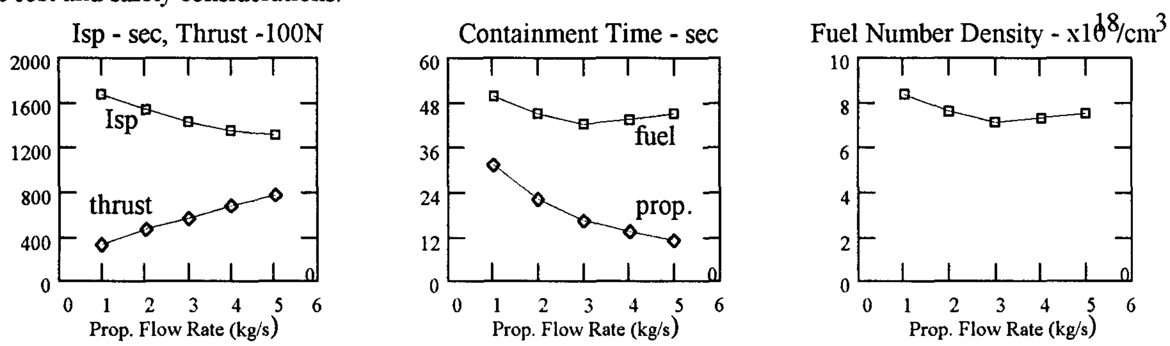

FIGURE 3. Propellant Mass Flow Rate Varied.

An increase in propellant mass flow rate also results in higher Isp and lower thrust. In this case the drop in specific impulse is due to the shorter containment time of the propellant, which leaves less time for the propellant to absorb energy. The fuel containment time and density plots show a minimum at 3 kg/s. As the propellant flow rate decreases below 3 kg/s, the propellant possesses less momentum which can be used to accelerate fuel, resulting in longer fuel containment times and densities. As the flow rate increases above 3 kg/s, the increase in propellant momentum is offset by the effect of the shorter propellant residence time, which does not allow ample time for propellant diffusion into the core. It is important to remember that the above results are for laminar flow only. If turbulence were to be modeled in this case, the increased propellant velocity associated with higher flow rates would no doubt promote additional mixing.

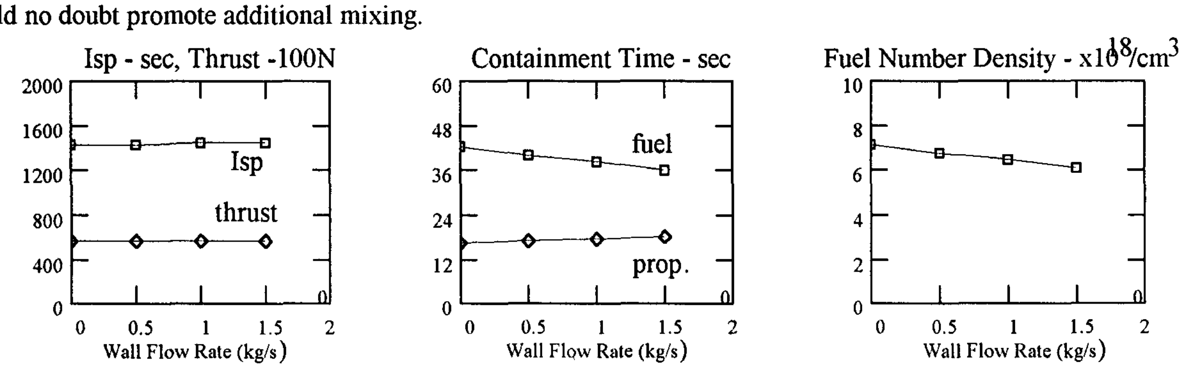

FIGURE 4. Wall Propellant Mass Flow Rate Varied.

In Figure 4, the total mass flow rate of the propellant is held constant at 3 kg/s; a wall flow rate of 1 kg/s results in an inlet flow rate of 2 kg/s. Also, the flow is perpendicular to the wall, and is uniformly distributed over the entire wall area. As the wall flow increases, the propellant residence time drops since the propellant has a shorter average distance to travel to the reactor exit (The residence time of propellant entering the reactor at the inlet is actually longer). The fuel residence time also drops as the wall flow rate is increased. As was discussed earlier, the mechanism which promotes the majority of fuel loss is the inward flow of hydrogen into the core. Inward propellant flow from the wall enhances this effect, thus resulting in less fuel containment. The only benefit of this additional mixing is a slightly higher Isp since more of the energy is being transferred to the propellant. In this case, turbulence modeling would benefit the designs with more wall flow because the velocity at the inlet is slower.

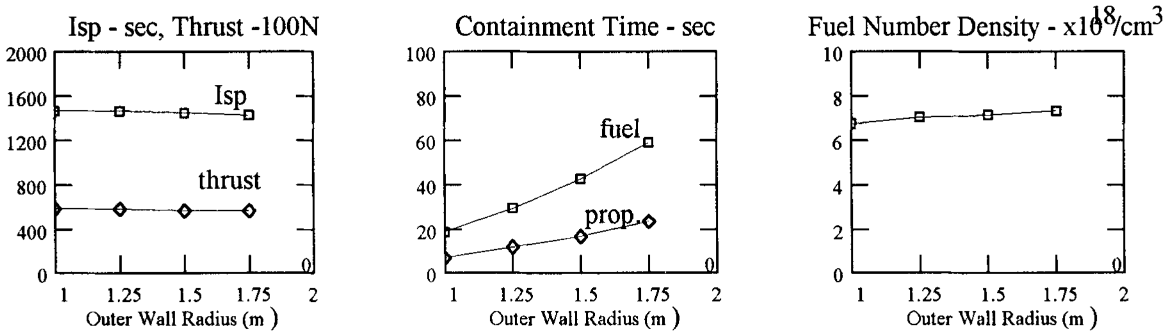

FIGURE 5. Outer Wall Radius Varied.

Increasing the reactor dimensions has two beneficial effects: velocities are slower, and gradients are spread out over a larger area. Therefore, the fuel and propellant containment times become substantially longer as the outer radius is increased. Unfortunately, the improvement in fuel number density isn't nearly as large. Considering the mass impact of increasing the radius, a smaller design is likely to be superior as long as the maximum wall heat flux can be avoided without pumping in excessive wall cooling flow.

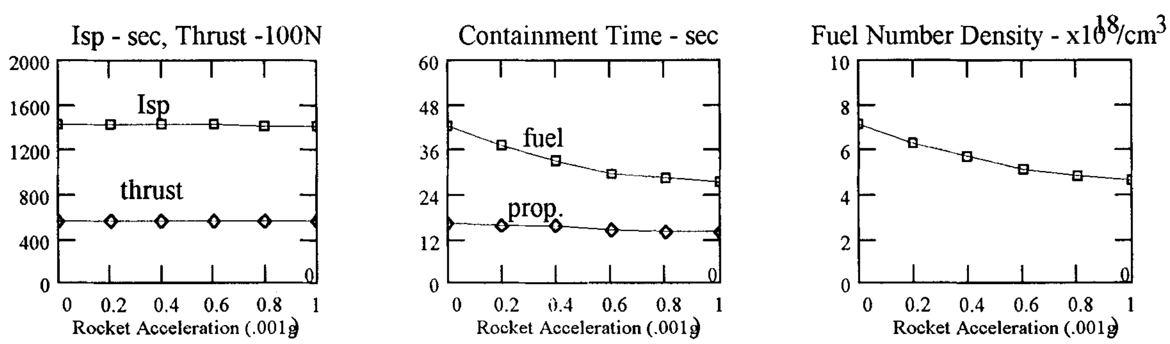

FIGURE 6. Axial Rocket Acceleration Varied.

Axial rocket acceleration is found to have an incredible effect on fuel containment. As rocket acceleration is increased, the buoyancy effects due to the large mass difference between uranium and hydrogen begin to dominate over all other forces. The fuel is accelerated quickly out of the reactor so that fuel/propellant mixing becomes insignificant. The buoyant forces are so powerful that an acceleration of only .001 g causes a recirculation region to appear between the fuel and propellant. The addition of an end wall could significantly improve fuel containment, but buoyancy effects would still be a problem.

To study how the momentum of the injected fluid effects containment, the injection velocity is varied (the area is varied for a constant mass flow). Increasing the radial momentum of the injected fluid causes the propellant to penetrate even further into the core region. This facilitates even more axial momentum transfer from the propellant to the fuel, resulting in less fuel containment. Also, the additional radial momentum of the propellant is not great enough to significantly compact the fuel; in fact the fuel hardly budges in the radial direction. Although not directly applicable, this raises the question of whether inward radial flow will be effective in containing the fuel in a spherical reactor. Changing the injection angle simply adds or subtracts to the axial momentum of the injected fluid, while the radial mass flow component remains unchanged. Injecting the wall flow at a negative angle (towards the inlet) enhances fuel/propellant mixing. For a wall flow of 1.5 kg/s, injection at -45° causes fuel containment to drop by 4%, and injection at +45° improves containment by 3%.

As mentioned in the Analysis section, the code offers many options for modeling turbulence. The characteristics of the above plots could change significantly depending on the turbulence model used. Frequent experimentation with the model has shown that the modeling of turbulence throughout the entire reactor is much more important than the turbulent modeling of fuel/propellant jet mixing near the inlet. When a constant eddy viscosity of $1E^{-5}$ is applied over the entire reactor, fuel containment drops by a factor of two.

CONCLUSIONS

A parametric analysis is performed which studies hydrodynamic fuel containment in a cylindrical open-cycle gas core nuclear rocket. In most cases, fuel containment is determined by the level of propellant convection into the core. Unfortunately, the parameter on which fuel containment is most dependent is power. Increasing the power from 500 MW to 1,000 MW causes fuel containment to drop by a factor of two. The effect of hydrodynamic forces due to wall injection are found to be minimal. The most significant finding of the study is the detrimental effect of rocket acceleration on fuel containment. An acceleration of only .001 g causes fuel containment to drop by 35%. Buoyancy effects could not only be a potential show-stopper for this design, but for other geometries and the nuclear light bulb concept as well.

Acknowledgments

All work was done at the University of Michigan. The work was sponsored by NASA Lewis Research Center as part of the NASA Graduate Researchers Program. The authors would like to acknowledge John Clark and Stan Borowski of NASA LeRC for their assistance.

References

Poston, D. I., and T. Kammash (1992) "Heat Transfer Model for an Open-Cycle Gas Core Nuclear Rocket," in *Proc. 9th Symposium on Space Nuclear Power Systems*, CONF-920104, M. S. El-Genk and M. D. Hoover, eds., American Institute of Physics, New York, AIP Conference Proc. No. 246, 3: 1083-1088.

Poston, D. I., and T. Kammash (1994) "A Comprehensive Thermal-Hydraulic Model of an Open-Cycle Gas Core Nuclear Rocket," in *Proc. 11th Symposium on Space Nuclear Power Systems*, CONF-940101, M. S. El-Genk and M. D. Hoover, eds., American Institute of Physics, New York.

Nomenclature

English

- a_p: Planck mean abs. (1/m)
- a_r: Rosseland mean abs. (1/m)
- C_p: Specific heat (J/kg·K)
- D_{12}: Binary diff. coef. (m^2/s)
- g: Acceleration (m/s^2)
- I_{sp}: Specific impulse (s)
- j: Diffusive flux ($kg/s{\cdot}m^2$)
- k: Thermal conduct. (W/m·K)
- m: Mass flow rate (kg/s)
- P: Pressure (Pa)
- q: Heat flux (W/m^2)
- Q_v: Heat generation (W/m^3)
- r: Radial position (m)
- T: Temperature (K)
- v: Local velocity (m/s)
- x: Fuel mole fraction
- y: Fuel mass fraction
- z: Axial position (m)

Greek

- μ: Viscosity (kg/m·s)
- ρ: Density (kg/m^3)
- σ: Stefan-Boltzmann Const.
- ψ: Dummy Variable

Subscript

- w: Outer wall